Derivation of the Resonant Frequency of Rectangular Dielectric Resonator Antenna by the Perturbation Theory

Saeed Fakhte and Homayoon Oraizi

Department of Electrical Engineering and Center of Excellence in Railway Transportation
Iran University of Science and Technology, Tehran, 16846-13114, Iran
saeedfakhte@elec.iust.ac.ir, h_oraizi@iust.ac.ir

Abstract ─ Based on the concept of perturbation theory, a modification to the dielectric waveguide model (DWM) is presented for the calculation of resonant frequency of rectangular dielectric resonator antenna (DRA). A large number of simulations are performed using commercial software and the results are compared between those of the DWM and the proposed method. Finally, the accuracy of proposed method is validated by the experimental data available in the literature. Differences between the measured and theoretical resonant frequencies vary by less than 2%.

Index Terms ─ Dielectric waveguide model, dielectric resonator antenna, perturbation theory, Q-factor, resonant frequency.

I. INTRODUCTION

Recently, dielectric resonator antennas (DRA) have received much attention owing to their numerous attractive characteristics, such as light weight, low profile and high radiation efficiency [1-6]. Rectangular shape is the most versatile due to its fabrication simplicity and improved degree of freedom compared to other shapes such as cylindrical or hemispherical shapes.

For the calculation of resonant frequencies and Q-factors of dielectric resonators, several methods have been reported. These methods include the closed cavity method with perfect magnetic conductor (PMC) walls [7], the dielectric waveguide model (DWM) [7], and the surface integral equation incorporated with the method of moments [8,9]. The perturbation correction to the DWM for characterizing the $TE^z_{01\delta}$ mode of cylindrical dielectric resonators has been reported [7]. This idea is used to improve the accuracy of DWM for estimating the resonant frequency of the rectangular DRA.

Various comparisons amongst the measured resonant frequencies and Q-factors of rectangular DRAs to those predicted using the dielectric waveguide model (DWM) have been carried out [10-12,14].

In this paper, the perturbation theory is applied to improve the accuracy of determination of the rectangular DRA resonant frequency using DWM. In fact, parts of stored electric and magnetic energies exist outside the DRA volume, which are neglected in the first-order DWM.

There are some differences between [7] and the proposed work. First, in [7] a cylindrical DRA is investigated whereas here a rectangular DRA is assumed. Second is that, in [7] a mode with non-broadside radiation pattern is studied and here a mode with broadside radiation pattern is examined. Observe that the Marcatili and EDC methods have already been used to improve the accuracy of DWM by using the electromagnetic fields outside the rectangular DRA [17]. However, the proposed method leads to more accurate results. The proposed perturbation method also provides an improvement for the calculation of Q-factor of rectangular DRAs. It is verified by comparison with the simulation and experimental data available in the literature.

II. THEORY

A rectangular dielectric resonator antenna (RDRA), whose dimensions are a×b×d/2 is located on a large ground plane (Fig. 1). The DRA has a relative dielectric constant of ε_r. By applying the image theory, the ground plane is removed and the procedure results in an isolated RDRA having dimensions $a \times b \times d$. The field components of TE^y_{111} mode inside the resonator have already been derived [18, Eq. (4)]. The resonance frequency f_o is obtained from the following transcendental equation [10]:

$$k_y \tan(\frac{k_y b}{2}) = \sqrt{(\varepsilon_r - 1)k_0^2 - k_y^2},$$

$$k_x^2 + k_y^2 + k_z^2 = \varepsilon_r k_0^2, \qquad (1)$$

$$k_x = \frac{\pi}{a}, k_z = \frac{\pi}{d},$$

where k_0 is the free space wave number at resonance frequency f_0 and other parameters are shown in Fig. 1.

Figure 2 shows a dielectric waveguide having a rectangular cross section of width a in the x-direction, height d in the z-direction with waves propagating in the y-direction. To model DRA, the waveguide is truncated

along the y-direction at $\pm b/2$.

To improve the model, the same electric and magnetic fields inside DRA (as for the first order DWM) are retained and the PMC walls are removed. The tangential electric fields at the resonator surfaces in the x- and z-directions are continuous. They exponentially decrease outside DRA in free space. Also, the fields in the dashed regions in Fig. 2 are assumed to be zero. The extended DRA model consists of five regions, as shown in Fig. 2.
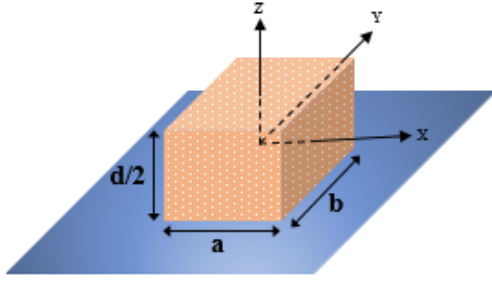

Fig. 1. 3D view of the isolated DR antenna configuration.
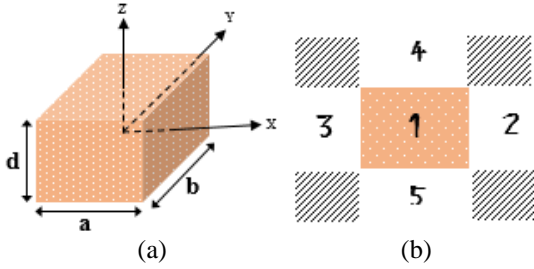

(a)   (b)

Fig. 2. (a) 3D view of the truncated dielectric waveguide model, and (b) cross-sectional view.

The fields outside the dielectric resonator must be of evanescent form. Therefore, the potential function of TE_{111}^y mode for $|x| > a/2$ takes the following form:

$$\psi_2^y = B \cos(k_y y)\cos(k_z z)e^{-\alpha_2 |x|}. \tag{2}$$

Then,

$$E_{x2,3} = -Bk_z \cos(k_y y)\sin(k_z z)e^{-\alpha_2 |x|}, \tag{3.a}$$

$$E_{y2,3} = 0, \tag{3.b}$$

$$E_{z2,3} = \pm B\alpha_2 \cos(k_y y)\cos(k_z z)e^{-\alpha_2 |x|}, \tag{3.c}$$

$$H_{x2,3} = \frac{\pm B\alpha_2}{j\omega\mu_0}k_y \sin(k_y y)\cos(k_z z)e^{-\alpha_2 |x|}, \tag{3.d}$$

$$H_{y2,3} = \frac{B(k_0^2 - k_y^2)}{j\omega\mu_0}\cos(k_y y)\cos(k_z z)e^{-\alpha_2 |x|}, \tag{3.e}$$

$$H_{z2,3} = \frac{Bk_y k_z}{j\omega\mu_0}\sin(k_y y)\sin(k_z z)e^{-\alpha_2 |x|}, \tag{3.f}$$

where

$$\alpha_2 = \sqrt{(\varepsilon_r - 1)k_0^2 - k_x^2}. \tag{4}$$

Also, for $|z| > d/2$ let,

$$\psi_4^y = C \cos(k_x x)\cos(k_y y)e^{-\alpha_4 |z|}. \tag{5}$$

Then,

$$E_{x4,5} = \mp C\alpha_3 \cos(k_x x)\cos(k_y y)e^{-\alpha_4 |z|}, \tag{6.a}$$

$$E_{y4,5} = 0, \tag{6.b}$$

$$E_{z4,5} = Ck_x \sin(k_x x)\cos(k_y y)e^{-\alpha_4 |z|}, \tag{6.c}$$

$$H_{x4,5} = \frac{Ck_x k_y}{j\omega\mu_0}\sin(k_x x)\sin(k_y y)e^{-\alpha_4 |z|}, \tag{6.d}$$

$$H_{y4,5} = \frac{C(k_0^2 - k_y^2)}{j\omega\mu_0}\cos(k_x x)\cos(k_y y)e^{-\alpha_4 |z|}, \tag{6.e}$$

$$H_{z4,5} = \frac{\pm Ck_y \alpha_3}{j\omega\mu_0}\cos(k_x x)\sin(k_y y)e^{-\alpha_4 |z|}, \tag{6.f}$$

where

$$\alpha_4 = \sqrt{(\varepsilon_r - 1)k_0^2 - k_z^2}. \tag{7}$$

In [18, Eq. (4)], the tangential components of the magnetic field are functions of $\cos(k_x x)$ and $\cos(k_z z)$, that vanish at $x=\pm a/2$ and $z=\pm d/2$ in agreement with the location of the PMC walls. On the other hand, the calculated H fields in the exterior regions consist of three components as H_x, H_y and H_z shown in Equations (3) and (6). The comparison of these components with those of [18, Eq. (4)], indicates that the tangential components of magnetic field are not continuous, whereas the transverse components are continuous. As an approximation, the tangential (XZ and YZ planes) components of magnetic field and transverse (XZ plane) components of electric fields in the exterior region are set equal to zero [7]. Also, as another approximation, it is assumed that the regions outside of the DR (regions 2, 3, 4 and 5) are bounded by PMC walls. The reason for this is that the energies in $(|y| > b/2, |x| > a/2)$ and $(|y| > b/2, |z| > d/2)$ regions are not considered in calculations. So, in $(|y| < b/2, |x| > a/2)$ and $(|y| < b/2, |z| > d/2)$ regions, $y=\pm b/2$ walls are considered as PMC walls. First, for calculation of the stored energies outside of the DRA, it is assumed that $k_y = n\pi/b$. Then, in the final formula the value of k_y which is obtained by DWM method was used. For an outward perturbation at a place of large electric field in a cavity, the resonant frequency increases [13].

The fields inside and outside the unperturbed DR cavity at the resonant frequency f_o are denoted by (E_{in}, H_{in}) and (E_{out}, H_{out}), respectively. Then,

$$\frac{f - f_0}{f_0} \approx \frac{\int_{\Delta v} (\mu|H_{out}|^2 - \varepsilon|E_{out}|^2)\,dv}{\int_{v_0} (\mu|H_{in}|^2 + \varepsilon|E_{in}|^2)\,dv}. \tag{8}$$

Equation (8) can be written in terms of stored energies as follows:

$$\frac{f - f_0}{f_0} = \frac{\Delta W_m - \Delta W_e}{W_m + W_e}, \tag{9}$$

where ΔW_m and ΔW_e are the changes in the stored magnetic energy and electric energy, respectively, due to the shape perturbation, and $W_e + W_m$ is the total stored energy in the DRA. In Equation (9), the numerator represents the difference of the stored magnetic and electric energies in regions 2, 3, 4 and 5, whereas the denominator represents the sum of both energies in region 1.

The integrals for the stored energies in separate regions can be calculated analytically:

$$\Delta W_m - \Delta W_e = \frac{\varepsilon_0 b(k_y^2 - k_0^2)}{16 k_0^2} A^2 \left[\frac{k_x^2 d}{\alpha_2} + \frac{k_z^2 a}{\alpha_4} \right], \tag{10}$$

$$W_e + W_m = \frac{\varepsilon_0 \varepsilon_r abd A^2}{16} (1 + \frac{\sin(k_y b)}{k_y b})(k_x^2 + k_z^2). \tag{11}$$

Substituting Equations (10) and (11) into Equation (9), we get:

$$f_{pert} = f_o + df, \tag{12}$$

where

$$df = f_o \frac{(\frac{k_y}{k_0})^2 - 1}{\varepsilon_r ad} \cdot \frac{1}{1 + \frac{\sin(k_y b)}{k_y b}}$$

$$\times \frac{\dfrac{k_x^2 d}{\sqrt{(\varepsilon_r - 1)k_0^2 - k_x^2}} + \dfrac{k_z^2 a}{\sqrt{(\varepsilon_r - 1)k_0^2 - k_z^2}}}{k_x^2 + k_z^2}. \tag{13}$$

Hence, by adding df to the resonant frequency calculated by DWM, the more accurate result for the resonant frequency of DRA can be obtained. Further, the radiation Q-factor of TE_{111}^y mode is determined in [10]:

$$Q_{rad} = \frac{\varepsilon_r \pi^4}{256(\varepsilon_r - 1)^2 k_0^5 abd}$$

$$\times \frac{1 + \sin c(k_y b)}{\sin c^2 (k_y b/2)} \cdot (k_x^2 + k_z^2). \tag{14}$$

The Q-factor accuracy can be improved by substituting the corrected theoretical value of resonant frequency, f_{pert}, in Equation (14) and is labeled Q_{pert}^{rad}.

III. RESULTS AND DISCUSSION

To examine the accuracy of the proposed method in predicting the resonant frequency and Q factor of an isolated rectangular DRA, the calculated resonant

frequencies were compared with the experimentally measured results in the literature, as well as with those computed from the eigenmode solver of ANSOFT HFSS 13. The eigenmode solver gives resonant frequency and field distribution of all the modes, which can be excited in DRA. Note that, in this solver the feed network is completely ignored. So, the results of the other simulation softwares, which consider the effects of the feed network (namely CST and HFSS driven modal), are slightly different from the eigenmode solvers. So, since the dielectric waveguide model (DWM) does not consider the effects of the feed network, the theoretical results should be compared with the eigenmode solvers.

Note that, the results of DRA excited by microstrip line and probe are affected by the presence of the feed and differ from the measured results of the isolated DRA. In Table 1, the theoretical and simulated results of resonant frequencies for TE_{111}^y mode of a DRA having dimensions b/a=0.5, d/a=0.9, and design resonant frequency f_o=5 GHz are presented, where the values of b/a, d/a, and resonant frequency are constant but the dielectric constant of the DRA varies.

The errors of the proposed modified model and the dielectric waveguide model (DWM) from the simulated resonant frequencies are denoted by:

$$\Delta f_{pert} = \frac{f_{pert} - f_{HFSS}}{f_{HFSS}}, \tag{15}$$

$$\Delta f_{DWM} = \frac{f_{DWM} - f_{HFSS}}{f_{HFSS}}, \tag{16}$$

$$\Delta f_{EDC} = \frac{f_{EDC} - f_{HFSS}}{f_{HFSS}}, \tag{17}$$

$$\Delta f_{Marc} = \frac{f_{Marc} - f_{HFSS}}{f_{HFSS}}, \tag{18}$$

where f_{HFSS} is the resonant frequency calculated by the Eigenmode solver of Ansoft HFSS, f_{DWM} is the resonant frequency calculated by DWM, f_{EDC} is the resonant frequency calculated by the EDC method, f_{Marc} is the resonant frequency calculated by the Marcatili method and f_{pert} is the resonant frequency calculated by the perturbation method. Observe that, the resonant frequencies calculated by DWM are lower than the simulated values by about 2% to 6.5%. The perturbational correction to DWM by the modified theoretical results are applied for the examples of Table 1. Observe that, the resonant frequencies calculated by the proposed model are more accurate than those of DWM, EDC and Marcatili. Also, the percentage difference between the calculated and simulated results of resonant frequencies and Q factors for both the DWM and the perturbation method are plotted in Fig. 3 (a) and defined as:

$$|\Delta f| = \frac{f_{calculated} - f_{simulation}}{f_{simulation}}, \tag{19}$$

$$|\Delta Q| = \frac{Q_{rad}^{calculated} - Q_{rad}^{HFSS}}{Q_{rad}^{HFSS}}. \quad (20)$$

Note that, the term "calculated" is referred to DWM and perturbation methods. The values of $|\Delta f|$ and $|\Delta Q|$ of TE_{111}^{y} mode of an isolated rectangular DRA are plotted versus b/a in Fig. 3 (a) for ε_r=90, d/a=0.6, and f_o=2.4 GHz and versus d/a in Fig. 3 (b) for ε_r=90, b/a=0.6, and f_o=2.4 GHz. The values plotted in Figs. 3 (b) and (c) have been computed for arbitrary but a high value of dielectric

constant, ε_r=90. Observe in Fig. 3 (b) that, as the value of the geometrical parameter b/a grows the differences between the results of DWM and simulations tend to be lower. $|\Delta f|$ for the perturbation method is always lower than that of DWM, but the $|\Delta Q|$ for DWM is more accurate for high values of b/a. Also, observe in Fig. 3 (b) that, for d/a>0.3 the results computed from the perturbation method are closer to the simulated results than those calculated by DWM.
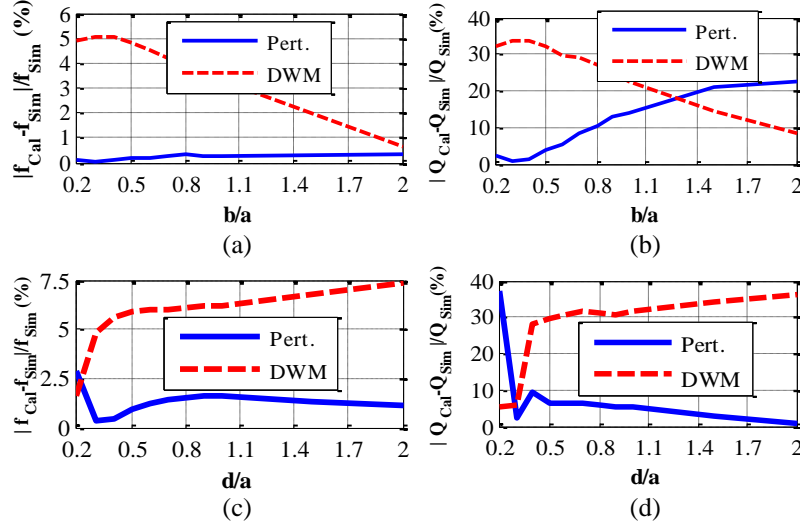

Fig. 3. The percentage difference between calculated and simulated resonant frequencies and Q factor versus: (a) aspect ratio, b/a, for ε_r=90, d/a=0.6, and f₀=2.4 GHz; (b) aspect ratio, d/a, for ε_r=90, b/a=0.6, and f₀=2.4 GHz.

Table 1: Theoretical and simulated resonant frequencies of TE_{111}^{y} mode of an isolated rectangular DRA. (b/a=0.5, d/a=0.9, f_{DWM}=5 GHz), frequency unit: GHz

ε_r	a (mm)	f_{DWM}	f_{HFSS}	f_{pert}	$f_{Marcatili}$	f_{EDC}	Δf_{DWM}	Δf_{pert}	$\Delta f_{Marcatili}$	Δf_{EDC}
10	17.75	5	5.102	5.2	4.82	4.71	-2%	1.9%	-5.53%	-7.68%
20	12.62	5	5.205	5.234	4.92	4.87	-3.9%	0.6%	-5.48%	-6.44%
30	10.33	5	5.255	5.245	4.95	4.91	-4.8%	-0.2%	-5.80%	-6.57%
40	8.95	5	5.28	5.25	4.96	4.93	-5.3%	-0.6%	-6.06%	-6.63%
50	8.01	5	5.301	5.253	4.97	4.95	-5.7%	-0.9%	-6.24%	-6.62%
60	7.31	5	5.317	5.255	4.97	4.96	-6%	-1.2%	-6.53%	-6.71%
70	6.77	5	5.325	5.257	4.98	4.96	-6.1%	-1.3%	-6.48%	-6.85%
80	6.34	5	5.334	5.258	4.98	4.97	-6.3%	-1.4%	-6.64%	-6.82%
90	5.98	5	5.338	5.259	4.98	4.97	-6.3%	-1.5%	-6.71%	-6.89%
100	5.67	5	5.346	5.259	4.98	4.97	-6.5%	-1.6%	-6.85%	-7.03%

These discrepancies between the results of DWM and simulation are due to the neglected stored energies outside the DRA volume. Figures 4 (a) and (b) show the ratio of the total stored energy outside (in regions 2-5) and inside the DRA, $(W_e + W_m)_{out}/(W_e + W_m)_{in}$, versus the geometrical parameters b/a, d/a, and ε_r, respectively.

Observing the stored energies ratio as a function of b/a, we conclude that increasing b/a decreases the exterior stored energies in an appreciable way. Thus, the

improvement of the accuracy of DWM for higher values of b/a (Fig. 3 (a)) is logical. When the parameter d/a is increased this energy ratio starts increasing (Fig. 4 (b)). Observe in Fig. 3 (b) that the error increase of DWM is expected.

Some experimental results for the resonant frequencies and Q factors of an isolated rectangular DRA are available [10,14, and 15]. To reveal the superiority of the proposed model over the first-order DWM, the errors

of these two models from measurement are considered in another example. In Table 2, the theoretical resonant frequencies and Q-factors calculated by the perturbation theory, DWM, EDC and Marcatili are compared with measured results. Observe that the corrected values of the resonant frequency and radiation Q-factor are much closer to the reported measured data. Differences between the measured and theoretical resonant frequencies vary between 0.47% to 1.94%. Also, the theoretical Q-factor may differ from the measured values from 2.74% to 8.82%.

The theoretical studies for arbitrary shaped antennas were focused on the bounds on the Q-factor of them. So, as our best knowledge, there is not any accurate closed form formula for determining the Q-factor of an arbitrary shaped dielectric antenna. For example, assuming that the DRA fabricated from a material of dielectric constant ε_r and has a radiation efficiency of 100%, then the Q-factor can be expressed by [19]:

$$Q = \frac{1 + 3(\frac{\pi}{\sqrt{\varepsilon_r}})^2}{(\frac{\pi}{\sqrt{\varepsilon_r}})^3 \left[1 + (\frac{\pi}{\sqrt{\varepsilon_r}})^2\right]}. \tag{21}$$

The calculated results by this formula are also listed in Table 2. Observe that, there are considerable difference

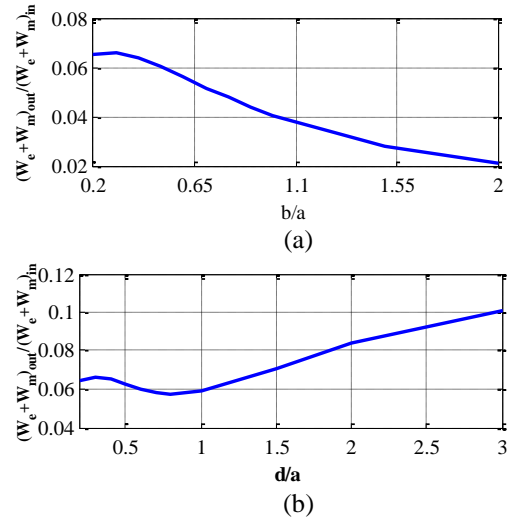between these results and those of measurement.

(a)

(b)

Fig. 4. The ratio of stored electric and magnetic energies in regions 2, 3, 4 and 5 to stored energies inside the DRA versus: (a) aspect ratio, b/a, for ε_r=90, d/a=0.6, and f_0=2.4 GHz; (b) aspect ratio, d/a, for ε_r=90, b/a=0.6, and f_0=2.4 GHz.

Table 2: Comparison of theoretical resonant frequency and radiation Q factor of rectangular DR with experimental results for TE_{111}^y mode of DRA. Frequency unit: GHz

	Ref.	[10]	[10]	[10]	[15]	[16]	[16]	[16]	[16]
Dimensions	ε_r	79.46	37.84	37.84	37.84	100	100	100	100
	a (mm)	7.45	8.6	8.77	8.6	10	10	12.7	10
	b (mm)	2.98	2.58	3.51	8.6	10	10	12.7	5
	d (mm)	7.45	8.6	8.77	2.58	4	2	2	2
Experiment	f_{exp}	4.673	6.322	5.684	10.28	4.57	7.97	7.72	8.5
	Q_{rad}^{Exp}	95	28.5	31.5	-	-	-	-	-
Perturbation	f_{per}	4.582	6.256	5.619	10.37	4.36	7.93	7.78	8.46
	Q_{rad}^{pert}	99.62	29.28	34.28	20.22	114.36	86.26	67.06	72.4
DWM	f_{DWM}	4.35	5.93	5.34	10.16	4.22	7.76	7.67	8.02
	Q_{DWM}^{rad}	128.9	37.98	44.07	17.14	105.3	37.28	24.57	60.6
Marcatili	f_{Marc}	4.33	5.9	5.30	9.75	4.18	7.58	7.43	7.9
EDC	f_{EDC}	4.31	5.84	5.26	9.75	4.17	7.58	7.43	7.9
Simulation	f_{sim}	4.647	6.28	5.65	10.14	4.38	7.83	7.65	8.42
Q_Bound	Q_{rad}^{Bound}	27.9	10.61	10.61	10.61	38.05	38.05	38.05	38.05
Error (%)	Δf_{DWM}	-7	-6.1	-6.1	-1.17	-7.7	-2.63	-0.65	-5.65
	ΔQ_{rad}^{DWM}	35.47	32.98	39.68	-	-	-	-	-
	Δf_{pert}	-1.94	-1.04	-1.14	0.88	-4.6	-0.5	0.78	-0.47
	ΔQ_{rad}^{pert}	4.86	2.74	8.82	-	-	-	-	-
	Δf_{Marc}	-7.34	-6.68	-6.76	-5.16	-8.54	-4.89	-3.76	-7.06
	Δf_{EDC}	-7.77	-7.62	-7.46	-5.16	-8.75	-4.89	-3.76	-7.06
	Δf_{sim}	-0.56	-0.67	-0.60	-1.37	-4.24	-1.77	-0.91	-0.95

To inspect the accuracy of the perturbation method in calculating the resonant frequency of a rectangular DRA compared to other methods, the calculated resonant frequencies were compared with the measured results, as well as those computed by the methods mentioned in the [17]. In this paper, a more comprehensive DWM method

reported that does not neglect fields outside of DRA. In Tables 3 and 4, the theoretical resonant frequencies of the samples calculated by the Marcatili method, EDC method [17], and proposed method and measured results are presented.

Note that, in [17] it has been mentioned that the TE_{mnl}^x mode of the structure is equivalent to the $TE_{m,2n-1,l}^x$ mode of an isolated resonator of height $2b$. Observe that, the resonant frequencies of fundamental modes calculated by the proposed method are generally more accurate than those of the Marcatili and EDC methods, but the results of EDC and Marcatili methods

for higher order modes are more accurate than those obtained by the proposed method. The results of the eigenmode solver of HFSS are also given in Table 4. Observe that, there is some difference between the results of simulation and measurement. This could be due to the effects of the feeding structure used in the experimental setup. However, the maximum error of the perturbation method is less than 6.5%. Comparison with the simulation results shows that the maximum error is even lower. Note that, the Marcatili and EDC methods [17] are taken into account the fields outside the DRA.

Table 3: Comparison of theoretical resonant frequency and radiation Q factor of rectangular DR with experimental results and the results of the [17]. a=d=6 mm, ε_r=37.1

Mode	b (mm)	Resonant Frequencies (GHz)						Difference with Experiment, %				
		DWM	Marcatili	EDC	Proposed	Sim.	Exp.	DWM	Marcatili	EDC	Proposed	Sim.
TE_{111}^y	4	6.96	6.89	6.86	7.27	7.32	7.27	-4.36	-5.2	-5.6	0	0.69
TE_{111}^x, TE_{111}^z	4	8	7.89	7.86	8.25	8.27	8.20	-2.47	-3.8	-4.1	0.61	0.85
TE_{111}^y	3	7.43	7.34	7.33	7.8	7.85	7.91	-6.26	-7.2	-7.3	-1.39	-0.76
TE_{111}^x, TE_{111}^z	3	9.72	9.52	9.46	10.01	9.95	9.97	-2.54	-4.5	-5.1	0.4	-0.20

Table 4: Comparison of theoretical resonant frequency of rectangular DR with experimental results and the results of the [17] for higher order modes. a=d=6 mm, ε_r=37.1

Mode	Dimension (mm)			Resonant Frequency (GHz)						Error (%)				
	a	2b	d	DWM	Prop.	Sim.	EDC	Marc.	Exp.	Δf_{DWM}	Δf_{pert}	Δf_{Sim}	Δf_{EDC}	$\Delta f_{Marc.}$
TE_{131}^x	12	20	8	8.66	8.69	8.44	8.41	8.45	8.30	4.24	4.59	1.67	1.32	1.79
TE_{131}^x	8	24	10	7.62	7.74	7.54	7.41	7.46	7.29	4.43	5.99	3.37	1.63	2.31
TE_{132}^x	8	20	12	10.21	10.28	10.03	9.99	10.02	9.7	5.12	5.81	3.35	2.95	3.25
TE_{132}^x	12	20	8	12.62	12.57	12.18	12.17	12.22	12.01	4.95	4.56	1.41	1.32	1.73
TE_{132}^x	10	24	8	12.25	12.25	11.85	11.68	11.80	11.62	5.28	5.28	1.96	0.51	1.54
TE_{132}^x	12	16	10	11.90	11.88	11.54	11.53	11.66	11.25	5.62	5.45	2.54	2.46	3.58
TE_{231}^x	8	20	12	10.52	11.08	10.84	10.31	10.43	10.40	1.15	6.33	4.14	-0.87	0.29
TE_{231}^x	8	24	10	10.11	10.74	10.52	9.91	10.02	10.25	-1.38	4.67	2.60	-3.37	-2.27
TE_{231}^x	12	16	10	10.6	10.96	10.70	10.28	10.43	10.40	1.9	5.24	2.84	-1.16	0.29

IV. CONCLUSION

In this paper the perturbation theory is applied to the dielectric waveguide model which is utilized for determining the resonant frequency and radiation Q factor of rectangular dielectric resonator antennas. The results obtained by this method are much closer to the simulated and measured ones compared to other reported methods.

REFERENCES

[1] S. Fakhte, H. Oraizi, and M. H. Vadjed-Samiei, "A high gain dielectric resonator loaded patch antenna," *Progress In Electromagnetics Research C*, vol. 30, pp. 147-158, 2012.

[2] S. Fakhte, H. Oraizi, R. Karimian, and R. Fakhte, "A new wideband circularly polarized stair-shaped dielectric resonator antenna," *IEEE Trans. Antennas Propag.*, vol. 63, no. 4, pp. 1828-1832, Apr. 2015.

[3] S. Fakhte, H. Oraizi, and R. Karimian, "A novel low cost circularly polarized rotated stacked dielectric resonator antenna," *IEEE Antennas and Wireless Propag. Lett.*, vol. 13, pp. 722-725, Apr. 2014.

[4] K. W. Leung, E. H. Lim, and X. S. Fang, "Dielectric resonator antennas: From the basic to the aesthetic," *Proc. IEEE*, vol. 100, no. 7, pp. 2181-2193, July 2012.

[5] A. Petosa and A. Ittipiboon, "Dielectric resonator antennas: A historical review and the current state of the art," *IEEE Antennas and Propagation Magazine*, vol. 52, no. 5, pp. 91-116, Oct. 2010.

[6] Q. Lai, G. Almpanis, C. Fumeaux, H. Benedickter, and R. Vahldieck, "Comparison of the radiation efficiency for the dielectric resonator antenna and the microstrip antenna at Ka band," *IEEE Trans. Antennas and Propag.*, vol. 56, no. 11, pp. 3589-

3592, 2008.

[7] D. Kajfez and P. Guillon, Eds., *Dielectric Resonators*. Artech House, Norwood, MA, 1986.

[8] A. W. Glisson, D. Kajfez, and J. James, "Evaluation of modes in dielectric resonators using a surface integral equation formulation," *IEEE Trans. Microwave Theory Tech*., vol. 31, pp. 1023-1029, 1983.

[9] A. A. Kishk, M. R. Zunoubi, and D. Kajfez, "A numerical study of a dielectric disk antenna above grounded dielectric substrate," *IEEE Trans. Antennas Propagat*., vol. 41, pp. 813-821, 1993.

[10] R. K. Mongia and A. Ittipiboon, "Theoretical and experimental investigations on rectangular dielectric resonator antennas," *IEEE Trans. Antennas Propag.*, vol. 45, no. 9, pp. 1348-1356, Sept. 1997.

[11] C. Trueman, et al., "Computation and measurement of the resonant frequencies and Q-factors of high permittivity dielectric resonators," *Symposium on Antenna Technology and Applied Electromagnetics ANTEM 94 Digest*, Ottawa, Canada, pp. 395-402, Aug. 1994.

[12] Y. M. M. Antar, D. Cheng, G. Seguin, B. Henry, and M. G. Keller, "Modified waveguide model (MWGM) for rectangular dielectric resonator antenna (DRA)," *Microwave and Optical Technology Letters*, vol. 19, no. 2, pp. 158-160, Oct. 1998.

[13] J. A. Kong, *Electromagnetic Wave Theory*. Wiley Interscience, 1990.

[14] C. W. Trueman, S. R. Mishra, C. L. Larose, and R. K. Mongia, "Resonant frequencies and Q factors of dielectric parallelepipeds," *IEEE Transactions Instrumentation and Measurement*, vol. 44, pp. 322-325, 1995.

[15] R. K. Mongia, A. Ittibipoon, and M. Cuhaci, "Low profile dielectric resonator antennas using a very high permittivity material," *Electron. Lett*., vol. 30, no. 17, pp. 1362-1363, 1994.

[16] Y. Liu, H. Liu, M. Wei, and S. Gong, "A low-profile and high-permittivity dielectric resonator antenna with enhanced bandwidth," *IEEE Antennas and Wireless Propag. Lett*., vol. 14, pp. 791-794, Mar. 2015.

[17] R. K. Mongia, "Theoretical and experimental resonant frequencies of rectangular dielectric resonators," *IEE Proc.-H*, vol. 139, pp. 98-104, 1992.

[18] S. Maity and B. Gupta, "Closed form expressions to find radiation patterns of rectangular dielectric resonator antennas for various modes," *IEEE Trans. Antenna and Propag*., vol. 62, no. 12, pp. 6524-6527, Oct. 2014.

[19] A. Petosa, *Dielectric Resonator Antenna Handbook*. Norwood, MA, Artech House, 2007.

Saeed Fakhte was born in Amlash, Iran, in 1987. He received the B.Sc. degree from the Sharif University of Technology, Tehran, Iran, in 2009, the M.Sc. degree from the Iran University of Science and Technology (IUST), Tehran, Iran, in 2012, and is currently working toward the Ph.D. degree in Electrical Engineering at IUST. Currently, he is a Visiting Scholar at the Politecnico di Torino, Torino, Italy. His research interests are in various areas of electrical engineering, such as dielectric resonator antenna design, metamaterials and the application of numerical methods in electromagnetics and antennas.

Homayoon Oraizi received the B.E.E. degree from the American University of Beirut, Beirut, Lebanon, in 1967, and the M.Sc. and Ph.D. degrees in Electrical Engineering from Syracuse University, Syracuse, NY, in 1969 and 1973, respectively. From 1973 to 1974, he was a Teacher with the K.N. Tousi University of Technology, Tehran, Iran. From 1974 to 1985, he was with the Communications Division, Iran Electronics Industries, Shiraz, Iran, where he was engaged in various aspects of technology transfer mainly in the field of HF/VHF/UHF communication systems. In 1985, he joined the school of Electrical Engineering, Iran University of Science and Technology, Tehran, Iran, where he is currently an Exemplary Professor of Electrical Engineering. From July 2003 to August 2003, he spent a two-month term as a Fellow of the Japan Society for the Promotion of Science with Tsukuba University, Ibaraki, Japan. From August 2004 to February 2005, he spent a six-month sabbatical leave at Tsukuba University. He has authored or co-authored over 300 papers in international journals and conferences. He has authored and translated several textbooks in Farsi. He was listed in the 1999 Who's Who in the World. His research interests are in the area of numerical methods for antennas, microwave devices, and radio wave propagation. Oraizi is a Fellow of the Electromagnetic Academy.